

See discussions, stats, and author profiles for this publication at: <https://www.researchgate.net/publication/267105711>

Self-Assembled Monolayers of Terminal Acetylenes as Replacements for Thiols in Bottom-Up Tunneling Junctions

ARTICLE *in* RSC ADVANCES · OCTOBER 2014

Impact Factor: 3.84 · DOI: 10.1039/C4RA09880C

CITATIONS

2

READS

41

4 AUTHORS, INCLUDING:



Davide Fracasso

National University of Singapore

7 PUBLICATIONS 125 CITATIONS

SEE PROFILE



Sumit Kumar

University of Groningen

1 PUBLICATION 2 CITATIONS

SEE PROFILE



Petra Rudolf

University of Groningen

256 PUBLICATIONS 5,667 CITATIONS

SEE PROFILE

CrossMark
click for updatesCite this: *RSC Adv.*, 2014, 4, 56026Received 5th September 2014
Accepted 17th October 2014

DOI: 10.1039/c4ra09880c

www.rsc.org/advances

Self-assembled monolayers of terminal acetylenes as replacements for thiols in bottom-up tunneling junctions†

Davide Fracasso,^{ab} Sumit Kumar,^a Petra Rudolf^a and Ryan C. Chiechi^{*ab}

Why use thiols in Molecular Electronics? They stink, oxidize readily, poison catalysts, and often require nontrivial protection/deprotection chemistry. In this communication we demonstrate the fabrication of tunneling junctions formed by contact of self-assembled monolayers (SAMs) of terminal alkynes onto silver and gold substrates. The SAMs form spontaneously upon exposure of the substrates to ethanolic solutions of the alkynes. Characterization by vibrational spectroscopy, XPS, and contact angles shows that the packing of the SAMs is nearly identical to those formed from equivalent thiols. Electrical characterization of the junctions revealed virtually no differences between SAMs on gold and silver, yielding $\beta_{Au} = 1.17 \pm 0.04 nC^{-1}$, $J_0 = (2.836 \pm 0.001) \times 10^3 A cm^{-2}$ for Au, and $\beta_{Ag} = 1.23 \pm 0.09 nC^{-1}$, $J_0 = (4.722 \pm 0.002) \times 10^3 A cm^{-2}$ for Ag. These values are in excellent agreement with junctions formed from alkanethiols of the same lengths as the alkynes, suggesting that there is no functional difference between thiols and alkynes as anchoring groups for SAMs. Yet alkynes are synthetically versatile, do not poison catalysts, are not odorous, and do not spontaneously oxidize, which are all attractive features for use in Molecular Electronics.

The strong, selective binding of organothiols to gold and other noble metals is widely exploited in Molecular Electronics (ME) to bind molecules to one or both electrodes in a device. Bottom-up tunneling junctions rely almost exclusively on self-assembled monolayers (SAMs) of thiols to define the gap between the electrodes.¹ Alkanethiols, in particular, are favored because they reproducibly form dense monolayers in a variety of conditions and tolerate a wide variety of head groups. The key feature of SAMs of thiols is the simultaneous strength and reversibility of the metal–thiol bond, which allows molecules to

self-assemble into dense monolayers that are sufficiently robust to support the application of a top-contact in a bottom-up device. Despite their popularity, there are significant disadvantages that are common to virtually all organothiols: they oxidize to disulfides under ambient conditions; their stench is detectable at concentrations of parts per billion and long term exposure can lead to permanent olfactory damage; and the reactivity of thiols and their tendency to poison catalysts can limit their synthetic accessibility and/or require the use of protecting groups that complicate or preclude synthetic efforts. Furthermore, in ME applications, the gold–thiolate interface introduces non-trivial complexities to modeling studies and acts as a barrier to charge transport from the involvement of sulphur 3d orbitals in bonding metals.^{2–4} Researchers in ME—particularly in top-down, single-molecule experiments—have explored alternative anchoring groups, such as isonitriles, aryl diazoniums, aryl iodoniums, and thiocyanates, dithiocarbamate, and selenium, but none have matched the facile, selective self-assembly of thiols that is required to form robust tunneling junctions in high yields.⁵ In this communication we suggest terminal alkynes as a drop-in replacement for thiols in bottom-up tunneling junctions composed of SAMs on gold and silver. Alkynes are an ideal replacement for three reasons: (i) they are synthetically accessible (and widely utilized in synthetic organic chemistry), (ii) they form carbon–metal bonds spontaneously, and (iii) they bind exclusively in an upright configuration *via* a σ interaction.⁶

Alkynes are known to have an affinity for and chelate with metals,^{7–11} but their self-assembly on surfaces had been thought to require the formation of acetylides electrochemically¹² or by deprotonation.¹³ Gorman and co-workers characterized SAMs formed by exposing solutions of *n*-alkyl terminal alkynes (acetylenes) in ethanol to gold, showing that alkynes spontaneously form densely packed monolayers analogously to thiols.¹⁴ However, while acetylides have been used in single-molecule ME devices (break-junctions),¹⁵ to the best of our knowledge, tunneling junctions based on the self-assembly of terminal alkynes—particularly into SAMs—have not been reported. We

^aStratingh Institute for Chemistry, University of Groningen, Nijenborgh 4, 9747 AG Groningen, The Netherlands. E-mail: r.c.chiechi@rug.nl; Fax: +31 (0)50 363 8751; Tel: +31 (0)50 363 7664

^bZernike Institute for Advanced Materials, University of Groningen, Nijenborgh 4, 9747 AG Groningen, The Netherlands

† Electronic supplementary information (ESI) available. See DOI: 10.1039/c4ra09880c

used eutectic Ga-In (EGaIn) as a top electrode¹⁶ to contact SAMs of *n*-alkyl terminal alkynes onto template-stripped¹⁷ gold (Au^{TS}) and silver (Ag^{TS}) and measure tunneling currents. We characterized the SAMs on Au^{TS} using surface enhanced Raman spectroscopy (SERS), attenuated total reflection (ATR) FT-IR, XPS, and contact angles to confirm the presence of the terminal alkynes on the surface (by comparison to Zhang *et al.*¹⁴) and the relative density of the monolayers. Further structural characterization of SAMs of alkynes on Au, including high-resolution scanning tunneling microscope images, is reported elsewhere.¹⁸

We performed Raman and attenuated total reflectance (ATR) measurements on neat 1-hexyne, 1-octyne, 1-decyne, and 1-dodecyne which we abbreviate AC6, 8, 10 and 12, respectively. All four alkynes clearly showed the expected $\nu(\text{C}\equiv\text{C})$ mode at 2118 cm^{-1} which corresponds to the alkyne stretching vibration. This vibration is expected to be weak for IR and strong for Raman (see Fig. S1 and S2 in the ESI† for ordinary Raman and FT-IR). While surface-enhanced Raman spectroscopy (SERS) studies have established that terminal alkynes bind to Au and Ag,^{19–21} the unambiguous characterization of SAMs of alkynes has only been performed on Au.^{14,18} Thus we first analyzed AC6–12 by SERS on roughened Au beads (see ESI† for experimental details). The resulting data, shown in Fig. 1, confirm the binding of all four alkynes to Au based on the $\sim 100\text{ cm}^{-1}$ red-shift in the alkyne stretching vibrations in the SER spectra, which occurs upon the adsorption/complexation of alkyne species to Au and Ag.^{6,8,9,11,19–21} These peaks (at $\sim 2000\text{ cm}^{-1}$ in Fig. 1) are broader than the Raman peaks due to the roughness of the polycrystalline surfaces of the gold beads and the presence of numerous defects induced by the Au surface reconstruction. Other peaks of interest are the CH_2 and CH_3 stretches at 2926 and 2955 cm^{-1} . These stretching modes can be used to compare the density of molecules and their packing, *i.e.*, the slight shift going from AC6 to AC12 is an indication of increasing order.²² The values are also within $\sim 1\text{ cm}^{-1}$ of asymmetric stretching modes in polycrystalline alkanethiols.²³ Furthermore, typical modes for alkanes are present at ~ 1450

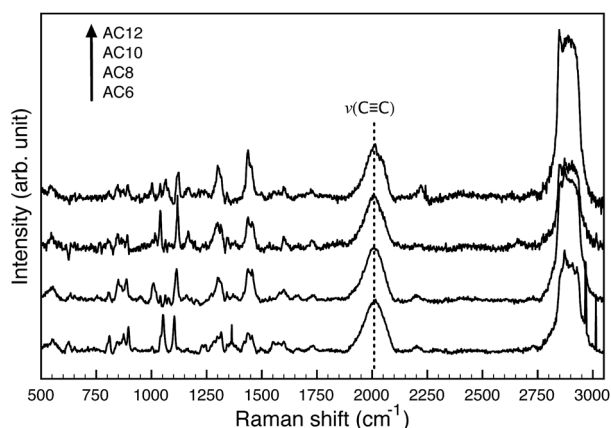


Fig. 1 SER spectra of AC6–12 SAMs on electrochemically roughened gold beads showing the characteristic peak for surface-bound alkynes.

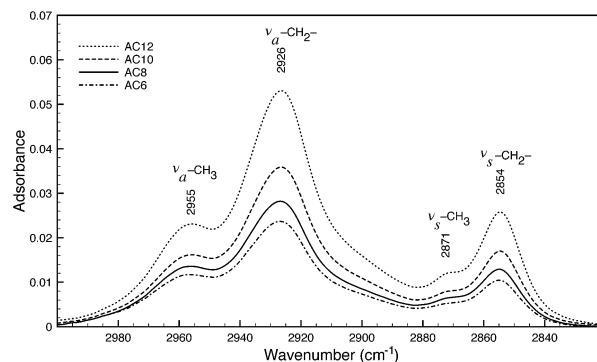


Fig. 2 ATR-IR of AC6–12 on Au^{TS} showing the characteristic methyl and methylene modes for *trans*-extended alkanes in a densely-packed monolayer. See ESI† for experimental details.

and $\sim 1300\text{ cm}^{-1}$, which we assign to scissoring vibrations of CH_2 .^{14,21}

We formed SAMs of AC6–12 by exposing 10 mM ethanolic solutions of the appropriate *n*-alkyl terminal alkyne to Au^{TS} and Ag^{TS} substrates for $\sim 20\text{ h}$ (see ESI† for details). To prove that densely-packed SAMs form on these ultra-smooth substrates, we measured the whole series on Au^{TS} by ATR-IR. An enlargement of this spectrum is shown in Fig. 2, showing the characteristic CH_2 and CH_3 peaks associated with *trans*-extended SAMs, see Fig. S3† for full spectra. The values of the peaks are within 1% of values reported for densely-packed SAMs of alkanethiols on Au, which is a strong indication that the alkyl portion of the SAMs studied in this work pack similarly to the equivalent thiol.²⁴ Taken together, the vibrational spectra unambiguously show the formation of ordered SAMs as depicted in Fig. 3. We observed the appearance of two peaks at 1740 and 1692 cm^{-1} respectively (see Fig. S4†). These modes could be attributed to aldehydes, however there is no evidence of oxidation of the alkynyl group on the surface. Oxidized carbon has been observed by XPS metal-bound acetylenes,^{12,13} however, it

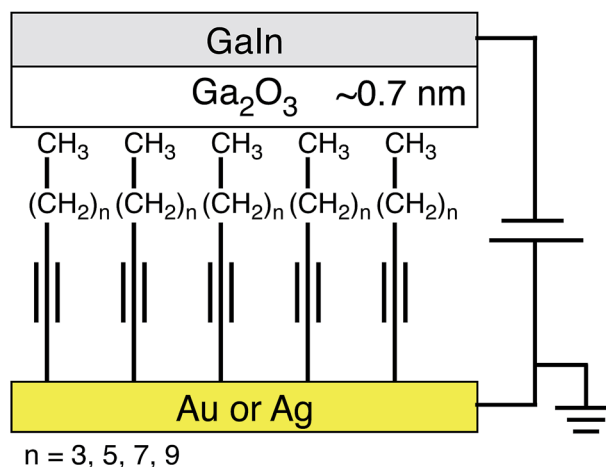


Fig. 3 A schematic of the tunneling junctions investigated; self-assembled monolayers of *n*-alkyl terminal alkynes on gold or silver are contacted with EGaIn bearing a $\sim 0.7\text{ nm}$ native oxide.

Table 1 Advancing contact angles measured for Milli-Q water on SAMs of AC6–12 on Au^{TS} and Ag^{TS}

SAMs	Au θ_{adv}^a	Ag θ_{adv}
AC6	80.1° (79°)	61.4°
AC8	89.7° (86°)	71.2°
AC10	91.2° (90°)	86.7°
AC12	98.7° (96°)	97.3°

^a Values from ref. 14 are shown in parentheses.

was not observed by Zhang *et al.* We performed XPS on AC12 (see ESI†) and found evidence of oxidized carbon species, however, some is also present in the bare Au^{TS} substrate. Nevertheless the relative ratio of sp³/sp is 4.8 : 1.0 which is consistent with previous results,¹⁴ and small impurities from oxidized carbon do not appear to affect tunneling transport or interfere with the stability and reproducibility of the resulting SAMs.

We compared the advancing water contact angles of SAMs of AC6–12 on Au^{TS} and Ag^{TS}, listed in Table 1, showing a clear angle increase with the increasing molecular length (*i.e.*, number of methylene units), which is an indication of increasing order in SAMs of alkanethiolates.²⁵ The values for SAMs of AC6–12 have been reported on Au surfaces (they are lower than for SAMs of alkanethiolates) and are in excellent agreement with our data,¹⁴ but they have not been reported on Ag. The contact angles are higher for Au^{TS} than Ag^{TS}, which suggests looser packing on Ag, however, in the absence of literature data against which to compare, we cannot draw any firm conclusions; the close agreement of the tunneling transport measurements, see Fig. 4 and 2, is strong evidence that there is little structural difference between SAMs of AC6–12 on Ag^{TS} and Au^{TS}, particularly in light of recent evidence of the sensitivity of EGaIn junctions to subtle differences in molecular packing.^{26,27}

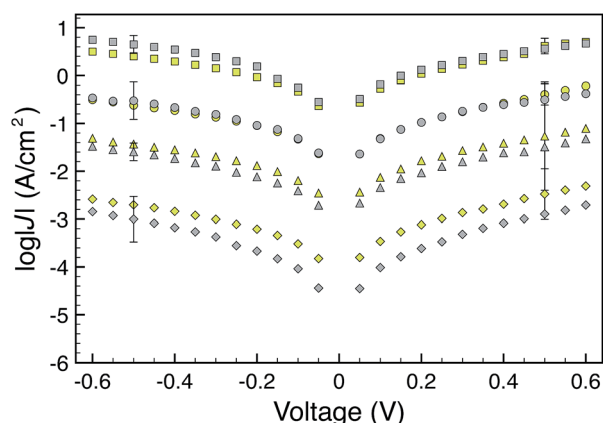


Fig. 4 Plots of current density (J) versus voltage (V) for SAMs of AC6 (squares), AC8 (circles), AC10 (triangles), and AC12 (diamonds) on Au^{TS} (yellow) and Ag^{TS} (grey) determined by fitting log-normal plots of J at each value of V to a Gaussian distribution. The error bars (shown on one point per trace for clarity) represent the variance.

Table 2 Number of J/V traces acquired and the % of junctions that did not fail during measurement (yield)

SAM	Traces		Yield	
	Au ^{TS}	Ag ^{TS}	Au ^{TS}	Ag ^{TS}
AC6	420	1140	100%	90%
AC8	800	528	92%	96%
AC10	660	3084	93%	80%
AC12	822	808	98%	98%

We constructed tunneling junctions of the SAMs of AC6–12 on Ag^{TS} and Au^{TS} by contact with sharp tips of EGaIn, sweeping through a potential range of ± 0.6 V, and collecting current-density *versus* voltage (J/V) plots at different positions on each of multiple substrates (Fig. 4). This procedure is described in detail elsewhere.^{28,29} We analyzed the resulting data by fitting a histogram of $\log J$ for each value of V to a Gaussian distribution. (See the ESI and Fig. S4 and S5† for experimental details and the histograms.) The symbols in Fig. 4 represent the Gaussian mean for the corresponding SAMs on Au^{TS} (yellow) and Ag^{TS} (grey). The error bars are the variance. The SAMs of AC6–12 behaved identically to alkanethiolates—they form robust junctions in high yields—thus we were able to treat the data identically. The conductances for AC6–12 on Ag^{TS} and Au^{TS} are within error of each other and are nearly indistinguishable. This remarkable similarity means that charge-transport most likely occurs through the backbones of the molecules and/or that the packing on Au^{TS} and Ag^{TS} is identical and that there is little, if any, difference in the binding modes on Ag and Au. The magnitude of J in Fig. 4 is also remarkably similar to SAMs of alkanethiolates with the same number of carbons.²⁷ This observation agrees with the observation that SAMs of carboxylic acids on AgO produce data indistinguishable from SAMs of thiols on Ag using EGaIn as a top contact.³⁰ Coupled with the observation that the identity of the head groups (*e.g.*, at the Ga₂O₃ interface) does not impact the rate of tunneling charge-transport^{31,32} we hypothesize that, although the carbon-metal bonds that anchor the SAMs of AC6–12 are probably less resistive than metal-thiolate bonds (and certainly CO₂H//AgO), the resistance of junctions composed of alkanes is dominated by the tunneling barrier formed from the carbon backbones and not the interfaces. The yields of working junctions, determined by the percentage of junctions that failed during a series of potential sweeps, and the total number of traces acquired for each SAM are shown in Table 2. The yields are in all cases excellent. The lowest yield is for AC10 on Ag^{TS}, which we compensated for by acquiring more scans on more junctions.

The different packing of SAMs of AC6–12 on Ag^{TS} as compared to Au^{TS} is apparent by the difference in advancing contact angles, which are systematically lower for Ag^{TS}. This trend may be apparent in Fig. 4. Although within error, the mean values of J for AC12, AC10, and AC6 are lower on Ag^{TS} than Au^{TS}. Since the yield of working junctions does not correlate with order in SAMs in EGaIn junctions³³ we can assume that the lower contact angles are the result of looser packing, but that

the molecules are still standing perpendicular to the substrate. Under this assumption there are simply fewer molecules in junctions (of the same area) formed on Ag^{TS}, which leads to smaller currents and hence lower average values of J . If we assume that the lower contact angles instead are a manifestation of disorder, then the lower values of J imply that disordered molecules are more resistive than those in ordered, densely packed regions of the SAMs. At the extreme of disorder, molecules are lying flat or nearly flat and the decrease in tunneling distance will cause an increase in J , however, small perturbations such as Gauche defects can maintain roughly the same tunneling distance while lowering the coupling between carbon atoms by distorting the σ framework (the hopping integral, t , in the sequential tunneling model³⁴). These explanations are purely speculative and do not account for the identical values of J for AC8, but it is possible to reconcile the lower contact angles of SAMs on Ag^{TS} with the observation that the yields and J/V properties are nearly indistinguishable.

The length-dependence of J for SAMs of n -alkanethiolates is well established as following Simmons' approximation, $J = J_0 e^{-d\beta}$, where d is the tunneling distance, J_0 is the theoretical value of J at $d = 0$, and β is the characteristic tunneling decay constant.³⁵ Values of β are often used to compare to or "validate" a method of measuring tunneling currents using values from the literature. Detailed statistical analyses of EGaIn/Ga₂O₃ junctions show that $\beta \approx 1 n_C^{-1}$ (i.e., per methylene unit; 0.8 \AA^{-1}) at 200–500 mV for SAMs of alkanethiolates,³⁶ which agrees well with literature values from various experimental techniques.^{27,37–40} There are no reported values of β (or tunneling junctions comprising SAMs) for alkynes against which to compare AC6–12, thus, to contextualize our data, we fit plots of $\ln J$ versus the total number of carbons in the alkynes (as opposed to inferring the molecular length). These data are shown in Fig. 5. We found $\beta_{\text{Au}} = 1.17 \pm 0.04 n_C^{-1}$, $J_0 = (2.836 \pm 0.001) \times 10^3 \text{ A cm}^{-2}$ for Au^{TS}, and $\beta_{\text{Ag}} = 1.23 \pm 0.09 n_C^{-1}$, $J_0 = (4.722 \pm 0.002) \times 10^3 \text{ A cm}^{-2}$ for Ag^{TS}. A comparison of these values to a range of values from the literature shows that β for both Au^{TS} and Ag^{TS} are in excellent agreement with reported values for SAMs of alkanethiolates measured using a variety of

Table 3 Comparison of values of β and J_0 to published values on thiolate SAMs

Substrate	$\beta \text{ } n_C^{-1}$	$\log J_0 \text{ A cm}^{-2} $
Au ^a	1.17 ± 0.04	4.45
Ag ^a	1.23 ± 0.09	4.67
Au ^b	0.76–1.10	2.0–8.9
Ag ^c	0.92–1.00	1.9–3.6

^a This work at 0.4 V. ^b Ref. 42 all electrodes at 0.5 V. ^c Ref. 42 only EGaIn at 0.5 V.

experimental techniques, which is further evidence that charges tunnel through the backbones of the molecules of the SAM and that the packing of the molecules is similar to that of alkanethiolates, i.e., that the alkyl portion is *trans*-extended. This comparison is summarized in Table 3. It has been shown that alkynes bind perpendicularly to Au through σ interactions and that the acidic acetylene proton is lost during this process.⁶ Our tunneling data imply that this binding mode is shared by both Au^{TS} and Ag^{TS}, which is also consistent with previous studies of ellipsometric thicknesses and electrochemical data on Au surfaces.^{14,41}

Values of J_0 are more difficult to compare than β , as they are reported less frequently and are more sensitive to experimental variations. However, our values are in good agreement, if not a bit higher, than those reported for EGaIn junctions comprising SAMs of alkanethiolates on Ag^{TS}.²⁷ Since J_0 reflects the theoretical value of J at $d = 0$, it can be thought of as the total contact resistance of a junction. The values of J_0 for AC6–12 on both Au^{TS} and Ag^{TS} are also in excellent agreement with values reported for SAMs of alkanethiols using a variety of other electrodes and techniques,⁴² (but slightly higher than those of partially-conjugated SAMs on Au^{TS} in EGaIn junctions).²⁹ This result implies that J_0 is dominated by the non-covalent interface between the Ga₂O₃ and the SAM, which is in agreement with impedance data.⁴³ If J_0 were dominated by the interface at the anchoring groups, it would differ for CO₂H//AgO, S–Au, S–Ag, C≡C–Au, and C≡C–Ag and the latter two would produce the lowest value by virtue of the better electronic coupling of C–metal bonds.

Further studies are necessary to establish the behavior of conjugated and more exotic molecular motifs in SAMs of alkynes, and to better understand the structure of AC6–12 on Ag^{TS}, but the data presented in this communication unambiguously show that SAMs of n -alkyl terminal alkynes can act as drop-in replacements for SAMs of alkanethiolates. In light of the myriad practical advantages of alkynes over thiols, why not use alkynes instead of thiols in Molecular Electronics?

Acknowledgements

We thank Oleksii Ivashenko and Wesley Browne for assistance with the Raman measurements. RCC also acknowledges the European Research Council for the ERC Starting Grant 335473 (MOLECSYNCON).

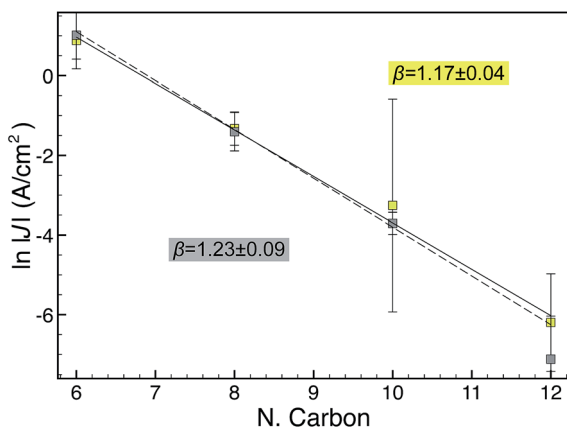


Fig. 5 Plots of $\ln J$ at 400 mV versus the number of carbons in the backbones of AC6–12 on Au^{TS} (yellow) and Ag^{TS} (grey). The insets show β (the negative slope).

References

- 1 Y. Zhang, Z. Zhao, D. Fracasso and R. C. Chiechi, *Isr. J. Chem.*, 2014, **54**, 513–533.
- 2 Y. Xue, S. Datta and M. A. Ratner, *J. Chem. Phys.*, 2001, **115**, 4292.
- 3 T. Ishida, M. Hara, I. Kojima, S. Tsuneda, N. Nishida, H. Sasabe and W. Knoll, *Langmuir*, 1998, **14**, 2092–2096.
- 4 H. Sellers, A. Ulman, Y. Shnidman and J. E. Eilers, *J. Am. Chem. Soc.*, 1993, **115**, 9389–9401.
- 5 E. Adaligil, Y.-S. Shon and K. Slowinski, *Langmuir*, 2010, **26**, 1570–1573.
- 6 P. Maity, S. Takano, S. Yamazoe, T. Wakabayashi and T. Tsukuda, *J. Am. Chem. Soc.*, 2013, **135**, 9450–9457.
- 7 N. J. Long and C. K. Williams, *Angew. Chem.*, 2003, **42**, 2586–2617.
- 8 M. L. Patterson and M. J. Weaver, *J. Phys. Chem.*, 1985, **89**, 5046–5051.
- 9 H. Feilchenfeld and M. J. Weaver, *J. Phys. Chem.*, 1989, **93**, 4276–4282.
- 10 J. Howard and Z. A. Kadir, *Zeolites*, 1984, **4**, 45–50.
- 11 D. C. Kennedy, C. S. McKay, L.-I. Tay, Y. Rouleau and J. P. Pezacki, *Chem. Commun.*, 2011, **47**, 3156–3158.
- 12 Q. Li, C. Han, M. Fuentes-Cabrera, H. Terrones, B. G. Sumpter, W. Lu, J. Bernholc, J. Yi, Z. Gai, A. P. Baddorf, P. Maksymovych and M. Pan, *ACS Nano*, 2012, **6**, 9267–9275.
- 13 A. M. McDonagh, H. M. Zareie, M. J. Ford, C. S. Barton, M. Ginic-Markovic and J. G. Matison, *J. Am. Chem. Soc.*, 2007, **129**, 3533–3538.
- 14 S. Zhang, K. Chandra and C. Gorman, *J. Am. Chem. Soc.*, 2007, **129**, 4876–4877.
- 15 W. Hong, H. Li, S.-X. Liu, Y. Fu, J. Li, V. Kaliginedi, S. Decurtins and T. Wandlowski, *J. Am. Chem. Soc.*, 2012, **134**, 19425–19431.
- 16 M. D. Dickey, R. C. Chiechi, R. J. Larsen, E. A. Weiss, D. A. Weitz and G. M. Whitesides, *Adv. Funct. Mater.*, 2008, **18**, 1097–1104.
- 17 E. A. Weiss, G. K. Kaufman, J. K. Kriebel, Z. Li, R. Schalek and G. M. Whitesides, *Langmuir*, 2007, **23**, 9686–9694.
- 18 T. Zaba, A. Noworolska, C. M. Bowers, B. Breiten, G. M. Whitesides and P. Cyganik, *J. Am. Chem. Soc.*, 2014, **136**, 11918–11921.
- 19 J. K. Lim, S.-W. Joo and K. S. Shin, *Vib. Spectrosc.*, 2007, **43**, 330–334.
- 20 B. K. Yoo and S.-W. Joo, *J. Colloid Interface Sci.*, 2007, **311**, 491–496.
- 21 Y. H. Jang, S. Hwang, J. J. Oh and S.-W. Joo, *Vib. Spectrosc.*, 2009, **51**, 193–198.
- 22 V. S. Dilimon, J. Denayer, J. Delhalle and Z. Mekhalif, *Langmuir*, 2012, **28**, 6857–6865.
- 23 P. E. Laibinis, G. M. Whitesides, D. L. Allara, Y. T. Tao, A. N. Parikh and R. G. Nuzzo, *J. Am. Chem. Soc.*, 1991, **113**, 7152–7167.
- 24 M. D. Porter, T. B. Bright, D. L. Allara and C. E. D. Chidsey, *J. Am. Chem. Soc.*, 1987, **109**, 3559–3568.
- 25 C. D. Bain, E. B. Troughton, Y. T. Tao, J. Evall, G. M. Whitesides and R. G. Nuzzo, *J. Am. Chem. Soc.*, 1989, **111**, 321–335.
- 26 N. Nerngchamnong, L. Yuan, D.-C. Qi, J. Li, D. Thompson and C. A. Nijhuis, *Nat. Nanotechnol.*, 2013, **8**, 113–118.
- 27 M. M. Thuo, W. F. Reus, C. A. Nijhuis, J. R. Barber, C. Kim, M. D. Schulz and G. M. Whitesides, *J. Am. Chem. Soc.*, 2011, **133**, 2962–2975.
- 28 D. Fracasso, H. Valkenier, J. C. Hummelen, G. C. Solomon and R. C. Chiechi, *J. Am. Chem. Soc.*, 2011, **133**, 9556–9563.
- 29 D. Fracasso, M. I. Muglali, M. Rohwerder, A. Terfort and R. C. Chiechi, *J. Phys. Chem. C*, 2013, **117**, 11367–11376.
- 30 K.-C. Liao, H. J. Yoon, C. M. Bowers, F. C. Simeone and G. M. Whitesides, *Angew. Chem.*, 2014, **126**, 3970–3974.
- 31 H. J. Yoon, C. M. Bowers, M. Baghbanzadeh and G. M. Whitesides, *J. Am. Chem. Soc.*, 2014, **136**, 16–19.
- 32 H. Yoon, N. Shapiro and K. Park, *Angew. Chem., Int. Ed.*, 2012, **124**, 4736–4739.
- 33 L. Yuan, L. Jiang, B. Zhang and C. A. Nijhuis, *Angew. Chem., Int. Ed.*, 2014, **53**, 3377–3381.
- 34 V. Mujica and M. A. Ratner, *Chem. Phys.*, 2001, **264**, 365–370.
- 35 J. G. Simmons, *Appl. Phys. Lett.*, 1963, **34**, 1793–1803.
- 36 W. F. Reus, C. A. Nijhuis, J. R. Barber, M. M. Thuo, S. Tricard and G. M. Whitesides, *J. Phys. Chem. C*, 2012, **116**, 6714–6733.
- 37 H. Song, Y. Kim, H. Jeong, M. A. Reed and T. Lee, *J. Phys. Chem. C*, 2010, **114**, 20431–20435.
- 38 W. Wang, T. Lee and M. Reed, *Phys. Rev. B: Condens. Matter Mater. Phys.*, 2003, **68**, 035416.
- 39 E. A. Weiss, R. C. Chiechi, G. K. Kaufman, J. K. Kriebel, Z. Li, M. Duati, M. A. Rampi and G. M. Whitesides, *J. Am. Chem. Soc.*, 2007, **129**, 4336–4349.
- 40 H. B. Akkerman and B. de Boer, *J. Phys.: Condens. Matter*, 2007, **20**, 013001–013021.
- 41 E. Z. Tucker and C. B. Gorman, *Langmuir*, 2010, **26**, 15027–15034.
- 42 F. C. Simeone, H. J. Yoon, M. M. Thuo, J. R. Barber, B. Smith and G. M. Whitesides, *J. Am. Chem. Soc.*, 2013, **135**, 18131–18144.
- 43 C. S. S. Sangeeth, A. Wan and C. A. Nijhuis, *J. Am. Chem. Soc.*, 2014, **136**, 11134–11144.